The p400 ATPase regulates nucleosome stability and chromatin ubiquitination during DNA repair

Ye Xu,[1] Yingli Sun,[1] Xiaofeng Jiang,[1] Marina K. Ayrapetov,[1] Patryk Moskwa,[1] Shenghong Yang,[1] David M. Weinstock,[2] and Brendan D. Price[1]

[1]Division of Genomic Stability and DNA Repair, Department of Radiation Oncology, and [2]Department of Medical Oncology, Dana-Farber Cancer Institute, Harvard Medical School, Boston, MA 02115

The complexity of chromatin architecture presents a significant barrier to the ability of the DNA repair machinery to access and repair DNA double-strand breaks (DSBs). Consequently, remodeling of the chromatin landscape adjacent to DSBs is vital for efficient DNA repair. Here, we demonstrate that DNA damage destabilizes nucleosomes within chromatin regions that correspond to the γ-H2AX domains surrounding DSBs. This nucleosome destabilization is an active process requiring the ATPase activity of the p400 SWI/SNF ATPase and histone acetylation by the Tip60 acetyltransferase. p400 is recruited to DSBs by a mechanism that is independent of ATM but requires mdc1. Further, the destabilization of nucleosomes by p400 is required for the RNF8-dependent ubiquitination of chromatin, and for the subsequent recruitment of brca1 and 53BP1 to DSBs. These results identify p400 as a novel DNA damage response protein and demonstrate that p400-mediated alterations in nucleosome and chromatin structure promote both chromatin ubiquitination and the accumulation of brca1 and 53BP1 at sites of DNA damage.

Introduction

DNA double-strand break (DSB) repair involves the deposition of DNA repair proteins onto the chromatin. Early events in the DNA damage response include the rapid recruitment of the ATM kinase to DSBs, followed by the phosphorylation of H2AX (γ-H2AX) on chromatin domains that extend for hundreds of kilobases on either side of the DSB (Bonner et al., 2008). The mdc1 scaffold protein then binds to γ-H2AX (Stucki et al., 2005), providing a docking platform for the deposition of DNA repair proteins onto the chromatin at DSBs (Melander et al., 2008; Spycher et al., 2008). Consequently, DSB repair can be negatively impacted by local chromatin architecture, which may restrict the ability of the DNA repair machinery to access and repair DSBs. Mammalian cells use multiple chromatin remodeling pathways to alter chromatin structure during DSB repair. For example, chromatin is hypersensitive to nuclease digestion after DNA damage (Smerdon et al., 1978; Carrier et al., 1999; Rubbi and Milner, 2003; Ziv et al., 2006), consistent with decompaction of a significant fraction of the chromatin in response to DSBs. This global decompaction requires the ATM-dependent phosphorylation of the kap1 heterochromatin-binding protein (Ziv et al., 2006), indicating that phosphorylation of kap1 may be essential for unpacking heterochromatin during DSB repair (Goodarzi et al., 2008). In addition to global effects on chromatin structure, biophysical studies indicate that there is a localized expansion of the chromatin adjacent to DSBs (Kruhlak et al., 2006), a process which was independent of the ATM kinase. These distinct pathways of chromatin remodeling indicate that cells use multiple mechanisms to create the open, accessible regions, which are critical for DSB repair.

Chromatin remodeling complexes contain SWI/SNF-related DNA-dependent ATPases, and use the energy of ATP hydrolysis to alter histone–DNA interactions, to reposition nucleosomes along the DNA (nucleosome sliding) or insert histone variants (Cairns, 2005). In yeast, the INO80, Swr1, and NuA4 complexes are recruited to enzymatically induced DSBs (Downs et al., 2004; van Attikum et al., 2004; Papamichos-Chronakis et al., 2006) and are required for DSB repair (van Attikum et al., 2004; Tsukuda et al., 2005). However, although mammalian

Correspondence to Brendan D. Price: brendan_price@dfci.harvard.edu

Abbreviations used in this paper: ChIP, chromatin immunoprecipitation; DSB, DNA double-strand break; IR, ionizing radiation; MEF, mouse embryo fibroblast; TSA, trichostatin A; ZFN, zinc finger nuclease.

The Rockefeller University Press $30.00
J. Cell Biol. Vol. 191 No. 1 31–43
www.jcb.org/cgi/doi/10.1083/jcb.201001160

cells exhibit alterations in chromatin structure during DSB repair (Rubbi and Milner, 2003; Kruhlak et al., 2006; Ziv et al., 2006), the mechanistic aspects of this process, including the protein complexes involved, the nature of the changes in chromatin structure, and how chromatin structure impacts DSB repair, are poorly understood. To gain insight into how chromatin remodeling contributes to DSB repair in mammalian cells, we examined the role of the p400 chromatin remodeler in regulating the stability of nucleosomes adjacent to DSBs. p400 is a SWI/SNF DNA-dependent ATPase (Chan et al., 2005) that functions to alter DNA–histone interactions and facilitates the insertion of histone variants, including H2A.Z, into gene promoters (Gévry et al., 2007). p400 is a component of the mammalian NuA4 complex (Downs et al., 2004; Doyon et al., 2004), and is associated with the Tip60 acetyltransferase. Tip60 is required for DSB repair (Bird et al., 2002; Sun et al., 2005, 2007, 2009; Murr et al., 2006; Gorrini et al., 2007), and can acetylate histones after DNA damage (Bird et al., 2002; Kusch et al., 2004; Murr et al., 2006; Jha et al., 2008). Further, p400 and Tip60 function in a common pathway to regulate apoptotic responses to DNA damage (Mattera et al., 2009), implying that the p400 ATPase and the Tip60 acetyltransferase may function to alter chromatin structure during DSB repair. Here, using DSBs generated by both genotoxic agents and by designer zinc finger nucleases to target a specific endogenous locus, we describe a new role for p400 in altering nucleosome stability during DSB repair.

Results

Histone–DNA interactions are very stable, and histones are only released from chromatin by NaCl concentrations in excess of 1.5 M (von Holt et al., 1989; Kimura and Cook, 2001; Shechter et al., 2007). If the stability of the histone–DNA interaction is reduced by DNA damage, it should be possible to preferentially elute histones from damaged chromatin by biochemical fractionation. To test this, cells were exposed to the radiomimetic agent bleomycin to introduce DSBs, and isolated nuclei were fractionated with increasing concentrations of NaCl and the histones in each fraction monitored (Fig. 1 a). Increasing the NaCl concentration from 0.2 to 0.6 M did not elute detectable amounts of histone from the chromatin. However, histones H2AX, γ-H2AX, H2B, H3, and H4 were released from bleomycin treated cells at 0.8–1.0 M NaCl, but not from untreated cells. At concentrations of NaCl of 1.5 M and above, disruption of histone–DNA interactions occurs (von Holt et al., 1989), as seen by release of histones from untreated cells at this concentration of NaCl (Fig. 1 a). This indicates that, after DNA damage, the interaction between histones and DNA in the chromatin is reduced, allowing histones to be extracted from the chromatin at lower levels of NaCl.

A key question is to determine the source of the fractionated histones. Changes in chromatin structure after DNA damage may be localized to regions adjacent to DSBs (Kruhlak et al., 2006) or associated with relaxation of the entire chromatin structure (Ziv et al., 2006). If the histones released by NaCl fractionation originate from DSBs, then, because the majority of γ-H2AX occurs at DSBs, the method should preferentially release γ-H2AX

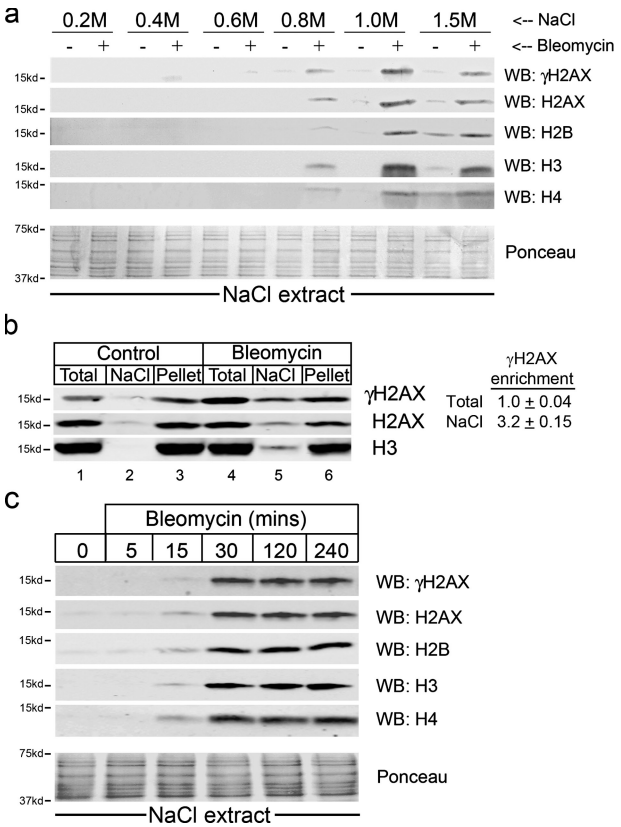

Figure 1. **DNA damage reduces the interaction between DNA and histones.** (a) 293T cells were exposed to 5 µM bleomycin for 30 min. Isolated nuclei were extracted in buffer containing the indicated concentration of NaCl. γ-H2AX, H2AX, H2B, H3, and H4 detected by Western blot. Membranes were stained with ponceau S to ensure equal loading. (b) 293T cells were untreated (control) or exposed to 5 µM bleomycin for 30 min. Total chromatin-associated histones were obtained by acid extraction. In parallel, cells were first extracted with 1.0 M NaCl and the nuclei collected by centrifugation. The histones remaining in the nuclear pellet were then purified by acid extraction. γ-H2AX, H2AX, and H3 were detected by Western blot. Table: Relative enrichment of γ-H2AX in the Total and NaCl extracts was calculated by normalizing γ-H2AX scan intensities to H2AX signal in each extract, expressed as $[\gamma\text{-H2AX}^{Total}]/[\text{H2AX}^{Total}]$ and $[\gamma\text{-H2AX}^{NaCl}]/[\text{H2AX}^{NaCl}]$. Results from three independent replicates, ± SD. (c) 293T cells were treated with 5 µM bleomycin and extracted in 1.0 M NaCl. γ-H2AX, H2AX, H2B, H3, and H4 were detected by Western blot. Equal loading confirmed by ponceau S staining.

from bleomycin-treated cells. In Fig. 1 b, nuclei were first extracted with 1.0 M NaCl (Fig. 1 b, lanes 2 and 5; NaCl fraction), the nuclei collected by centrifugation, and the histones remaining in the nuclear pellet extracted by acid extraction (Fig. 1 b, lanes 3 and 6; Pellet). For comparison, total histones (obtained by acid extraction) are shown (Fig. 1 b, lanes 1 and 4; Total). Control cells contained low but detectable levels of γ-H2AX (lane 1). No detectable γ-H2AX, H2AX, or H3 was seen after fractionation of control cells in 1.0 M NaCl (Fig. 1 b, lane 2), indicating that this pool of γ-H2AX remains associated with the chromatin (lane 3). In contrast, bleomycin treatment led to the elution of low but detectable levels of histones H2AX and H3 (compare lanes 4 and 5). γ-H2AX levels were increased by bleomycin (compare lanes 1 and 4), and a significant fraction of this γ-H2AX was released by NaCl fractionation (lane 5). Importantly, although only a small fraction of the total H2AX was eluted

by NaCl after bleomycin treatment, this eluted fraction was significantly enriched for γ-H2AX compared with the total (Fig. 1 b, lane 5). To determine the exact enrichment of γ-H2AX, Western blots were quantitated (Fig. S1 a), and the levels of γ-H2AX normalized to the level of H2AX in each extract. NaCl-extracted histones contained 3.2-fold more γ-H2AX compared with the overall amount in the total chromatin (Fig. 1 b, table). The histones extracted from the chromatin by NaCl after DNA damage are therefore enriched for γ-H2AX, indicating that they preferentially originate from regions of the chromatin containing high levels of γ-H2AX—that is, from chromatin regions adjacent to the DSBs. However, we cannot exclude the possibility that a fraction of the released histones are derived from chromatin domains that are not associated with the DSB.

Next, we monitored the time course of changes in histone–DNA interaction after DNA damage. Histone sensitivity to NaCl fractionation was detected 15–30 min after bleomycin addition (Fig. 1 c), and was maintained for at least 4 h during continuous bleomycin exposure. In contrast, acute exposure to ionizing radiation (IR) induced a more limited chromatin response, such that the chromatin-associated histones were only sensitive to NaCl fractionation for ∼30 min after irradiation (Fig. 2 a). The destabilization of the chromatin in response to acute DNA damage (IR) is therefore an early but transient response to DSBs.

The decrease in the stability of histone–DNA interactions was only detected 15 min after DSB production (Fig. 1 c and 2 a), whereas ATM activation and phosphorylation of H2AX were maximal within 5 min of exposure to IR (Fig. 2 b). Because the altered DNA–histone stability occurs after ATM activation, we determined if it was regulated by the ATM kinase. Both *A-T* cells (which lack ATM protein) and *A-T* cells complemented with ATM (*A-T*^{ATM}; Sun et al., 2005, 2009) had similar sensitivity to NaCl extraction after exposure to bleomycin (Fig. 2 c). In addition, neither inhibition of ATM kinase by Ku55933 (Hickson et al., 2004; Fig. 2 d and Fig. S1 b) nor inactivation of the MRN complex (Fig. S1), which regulates ATM (Lee and Paull, 2005), blocked the reduced histone–DNA interaction seen after DSB production (Fig. S1 d). Previous work demonstrated that global chromatin relaxation required phosphorylation of kap-1 by ATM (Ziv et al., 2006). However, the reduced stability of DNA–histone interactions seen after DNA damage was independent of both ATM and kap1 phosphorylation (Fig. S1 b). The localized changes in chromatin structure reported here are therefore mechanistically distinct from the changes in chromatin structure mediated by the ATM-kap1 pathway (Ziv et al., 2006). The results are consistent with a model in which, immediately after DNA damage, the chromatin structure at or near DSBs is altered, weakening the interaction between DNA and histones, and therefore allowing histones to be released from the chromatin in 1.0 M NaCl. We refer to this reduction in histone–DNA interaction after DNA damage as reduced nucleosome stability.

The Tip60 (Gorrini et al., 2007; Sun et al., 2009) and Trrap (Murr et al., 2006; Robert et al., 2006) subunits of the NuA4 complex have been implicated in DSB repair (Downs et al., 2004; Doyon et al., 2004). Here, we examined if the p400 SWI/SNF ATPase subunit of NuA4 was required for the decrease in nucleosome stability at DSBs. When p400 was reduced by shRNA

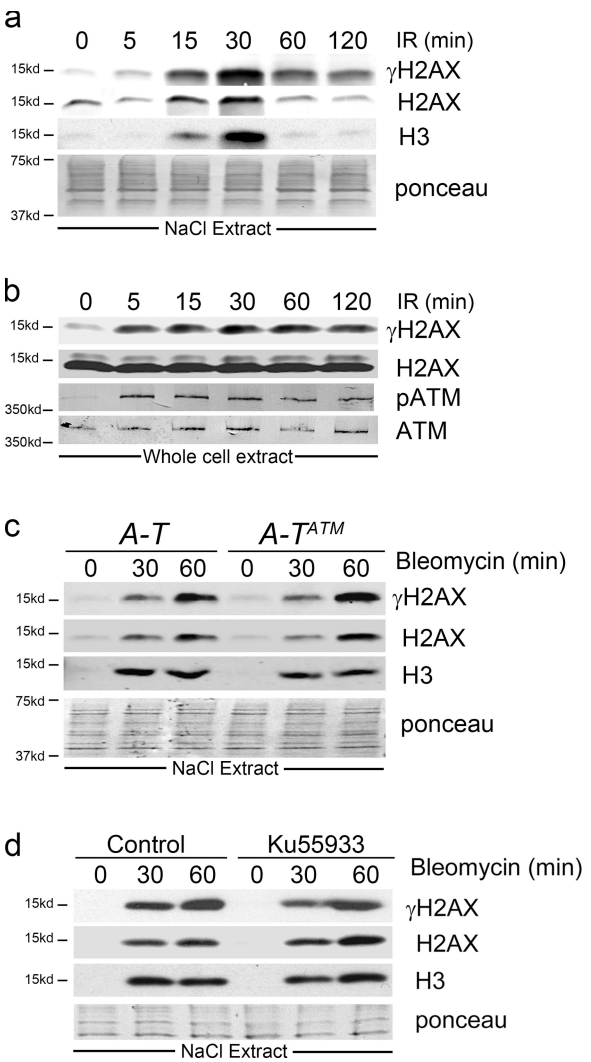

Figure 2. **ATM is not required for altered nucleosome stability after DNA damage.** (a) 293T cells were irradiated (10Gy), fractionated in 1.0 M NaCl, and released histones detected by Western blot. (b) 293T cells were irradiated (10Gy) and whole-cell extracts examined by Western blot for total γ-H2AX, H2AX, ATM, and pATM. (c) GM5849 A-T cells complemented with either vector (*A-T*) or full-length ATM (*A-T*^{ATM}) were exposed to 5 μM bleomycin, fractionated in 1.0 M NaCl, and released histones detected by Western blot. (d) 293T cells were incubated with 10 μM of the ATM kinase inhibitor Ku55933 for 60 min, followed by 5 μM bleomycin. Cells were fractionated in 1.0 M NaCl, and released histones detected by Western blot.

(see Fig. 6 c), no histones were eluted from bleomycin-treated cells by NaCl treatment (Fig. 3 a), indicating that p400 is required to reduce nucleosome stability after DNA damage. If p400 functions as part of the NuA4 complex, loss of the Trrap subunit, which is thought to function as a scaffold protein for the NuA4 complex, should also impact nucleosomal remodeling. Indeed, when Trrap levels were reduced with shRNA (Fig. S2 b), the ability of NaCl fractionation to release histones from the chromatin was lost (Fig. 3 b), demonstrating that Trrap is required for reducing nucleosome stability. Chromatin remodeling is facilitated by acetylation of histones, which can reduce the stability of histone–DNA interaction and inhibit the packing of nucleosome arrays (Brower-Toland et al., 2005; Dion et al., 2005;

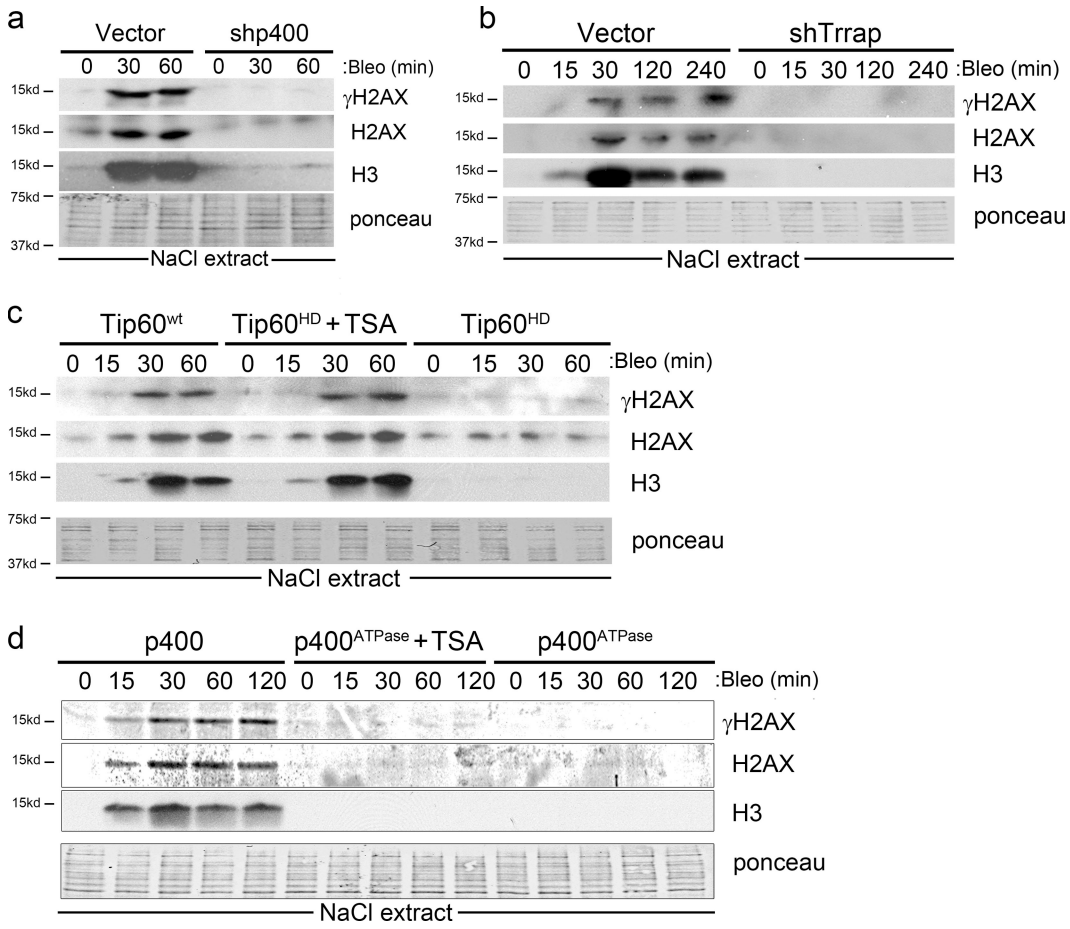

Figure 3. **Tip60, p400, and Trrap are required for altered nucleosome stability.** (a) 293T cells expressing a nonspecific shRNA (vector) or shRNA targeting p400 were exposed to 5 µM bleomycin. Cells were fractionated in 1.0 M NaCl, and released histones detected by Western blot. (b) HeLa cells expressing vector or shRNA targeting Trrap were exposed to bleomycin. Cells were fractionated in 1.0 M NaCl, and released histones detected by Western blot. (c) 293T cells expressing either HA-Tip60 or catalytically inactive HA-Tip60^{HD} were incubated with 5 µM bleomycin. Cells were fractionated in 1.0 M NaCl, and released histones detected by Western blot. Where indicated, cells were pretreated with 300 nM TSA for 2 h. (d) 293T cells expressing either HA-p400 or HA-p400^{ATPase} were incubated with 5 µM bleomycin. Cells were fractionated in 1.0 M NaCl, and released histones detected by Western blot. Where indicated, cells were pretreated with 300 nM TSA for 2 h.

Shogren-Knaak et al., 2006; Choi and Howe, 2009). The Tip60 acetyltransferase associates with NuA4 and acetylates H4 after DNA damage (Kusch et al., 2004; Murr et al., 2006; Jha et al., 2008), suggesting that Tip60 may regulate nucleosome stability. Cells expressing a previously described catalytically inactive version of Tip60 (Tip60^{HD}; Fig. S2c; Sun et al., 2005) lacked any detectable decrease in nucleosome stability after DNA damage (Fig. 3 c), indicating that Tip60's acetyltransferase activity is required for alteration of nucleosome stability after DNA damage. To confirm that histone acetylation is crucial, Tip60^{HD} cells were pretreated with the histone deacetylase inhibitor trichostatin A (TSA). TSA increased H4 acetylation levels (Fig. S2 d) and restored the ability of bleomycin to decrease nucleosome stability in the Tip60^{HD} cells (Fig. 3 c). Hyperacetylation of histones through histone deacetylase inhibition therefore compensates for the loss of Tip60's acetyltransferase activity, demonstrating that histone acetylation by Tip60 is required for reduced nucleosomal stability at DSBs.

p400 and Trrap are integral components of NuA4 (Doyon et al., 2004). Reducing p400 or Trrap with shRNA may disassemble NuA4, making it difficult to determine if the observed effects are due to loss of p400 or loss of the entire NuA4 complex. To distinguish between these possibilities, p400's ATPase activity was inactivated by mutagenesis (Samuelson et al., 2005). Cells expressing wild-type p400 (Fig. S2 a) showed decreased nucleosome stability after bleomycin treatment, whereas this effect was lost in cells expressing the p400^{ATPase} mutant (Fig. 3 d). Similar results were seen after IR exposure (Fig. S2 a). In addition, preincubation of the p400^{ATPase} cells with TSA to induce histone hyperacetylation did not restore the ability of bleomycin to decrease nucleosome stability (Fig. 3 d). Histone acetylation, on its own, is therefore insufficient to decrease nucleosome stability at DSBs. Fig. 3 demonstrates that both Tip60's acetyltransferase activity and p400's ATPase activity are required for regulating nucleosome stability at DSBs. Further, because p400, Tip60, and Trrap are components of the mammalian NuA4 complex (Doyon et al., 2004), it is likely that these proteins regulate DSB repair as part of the NuA4 complex.

Next, the role of p400 in the DNA damage response was investigated. Fig. 4 a demonstrates that p400^{ATPase} cells are significantly more sensitive to ionizing radiation than cells expressing wild-type p400. Cells expressing the p400^{ATPase} also exhibited

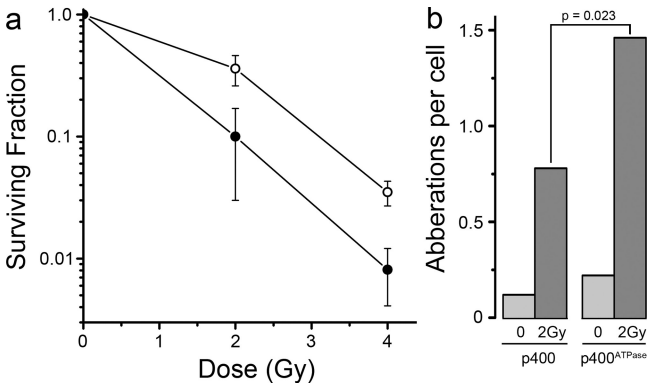

Figure 4. **Loss of p400's ATPase activity increases radiosensitivity and chromosome aberrations.** (a) HeLaS3 cells expressing either p400 (○) or p400^{ATPase} (●) were irradiated, and the number of surviving colonies measured 12 d later. Each data point represents the average of three independent assays, results ± SD. (b) p400 or p400^{ATPase} cells were untreated (0) or irradiated (2Gy) and allowed to recover for 14 h. Metaphase spreads were subsequently scored visually for chromosome aberrations. Results expressed as aberrations per cell (n = 50 cells), and P values determined using t test.

a more rapid exit from G2 arrest than control cells (Fig. S2 e), consistent with a small defect in G2 arrest in these cells. In addition, irradiation of the p400^{ATPase} cells resulted in significantly higher levels of chromosome aberrations compared with cells expressing wild-type p400 (Fig. 4 b). These observations are consistent with a significant DNA repair defect in the p400^{ATPase} cells, and define p400 as a novel DNA damage response protein that is required for cells to survive exposure to IR.

Although many DNA damage responses form foci at DSBs, we were unable to detect p400 foci using immunofluorescent approaches. Accordingly, we used an alternative, chromatin immunoprecipitation (ChIP)–based approach to monitor recruitment of p400 to DSBs. Zinc finger nucleases (ZFN) are custom-engineered nucleases in which the catalytic domain of the Fok1 endonuclease is linked to an engineered zinc finger protein, creating sequence-specific nucleases that generate a DSB at unique chromatin sites (Urnov et al., 2005). DSBs caused by ZFNs at endogenous loci in human cells can be used to insert or alter genomic sequences through homology-directed repair with donor DNA (Urnov et al., 2005; Hockemeyer et al., 2009), and have been used to examine chromosomal translocations (Brunet et al., 2009). The AAVS1 ZFN (p84-ZFN) introduces a single DSB into intron 1 of the *PPP1R12C* gene on chromosome 19 (Hockemeyer et al., 2009). p84-ZFN was used to introduce a single DSB into chromosome 19, and ChIP analysis was then used to monitor p400 recruitment to this unique DSB. Transient transfection of the p84-ZFN generates DSBs in 40–50% of cells into which it is introduced (Fig. 5 a and Fig. S3 b). The ZFN-generated DSB increases the levels of γ-H2AX (Fig. S3 a), and ChIP analysis demonstrates the formation of γ-H2AX domains extending at least 3.5 kb on either side of the ZFN DSB (Fig. 5 b). Significantly, ChIP analysis demonstrated that p400 was also recruited to chromatin domains adjacent to the DSB (Fig. 5 c), indicating that p400, like other DNA damage response proteins, is actively recruited to and retained at DSBs. Next, we examined if the decreased nucleosome stability mediated by p400 could be detected using the ZFN ChIP approach. p400 and p400^{ATPase} cells were transfected with the ZFN nuclease to create DSBs, and then extracted in 1.0 M NaCl to remove histones from regions of decreased nucleosome stability. ChIP was then performed using an anti-H3 antibody to look for depletion of H3 on the chromatin adjacent to the ZFN site on chromosome 19. For comparison, we examined a randomly selected region on chromosome 6. Histone H3 was specifically removed from the chromatin adjacent to the ZFN DSB by NaCl extraction (−1.5 kb; Fig. 5 d, *Chr19*) in wild-type cells, but not in p400^{ATPase} cells. In contrast, no significant release of H3 was detected at an unrelated region on chromosome 6 (Fig. 5 d, Chr 6). This is consistent with the results in Fig. 1 b, and supports the proposal that the decrease in nucleosome stability is preferentially localized to chromatin domains adjacent to the DSB on chromosome 19.

One potential explanation for the inability of the p400^{ATPase} protein to alter nucleosome stability is that it is not recruited to DSBs. However, Fig. 6 a demonstrates that both p400 and the p400^{ATPase} proteins were recruited to DSBs with similar efficiency. In addition, p400 was recruited to DSBs in Tip60^{HD} cells (Fig. 6 a). Thus, the inability of the p400^{ATPase} and Tip60^{HD} mutants to decrease nucleosome stability (Fig. 3) is not due to the failure to recruit these proteins to DSBs, but to the lack of intrinsic catalytic activity. Tip60 acetylates histone H4 after DNA damage (Bird et al., 2002; Murr et al., 2006), suggesting that Tip60 may regulate nucleosome stability through acetylation of histone H4. ChIP analysis confirmed that H4 acetylation was increased in cells with ZFN-induced DSBs, but not in cells expressing the catalytically inactive Tip60^{HD} (Fig. 6 b). We also examined if the ability of Tip60 to acetylate histones at DSBs requires p400's ATPase activity. Fig. 6 b demonstrates that, although histone H4 was acetylated after DSB generation in wild-type p400 cells, H4 acetylation was slightly reduced in cells expressing the p400^{ATPase} mutant. Because p400 and Tip60 are part of the NuA4 complex, it is possible that the p400^{ATPase} mutant affects the intrinsic catalytic activity of Tip60. Fig. 6 c (inset) demonstrates that p400 and Tip60 are specifically coprecipitated from cells, as previously shown (Doyon et al., 2004), and that the p400–Tip60 interaction was not altered by DNA damage (Fig. 6 c). Next, p400 was immunopurified and the associated acetyltransferase activity measured as we previously described (Sun et al., 2005). The acetyltransferase activity associated with immunopurified p400 was increased by DNA damage (Fig. 6 c); cells expressing shRNA to p400 or immunopurification with IgG exhibited little or no associated acetyltransferase activity or Tip60. Significantly, the catalytically inactive p400^{ATPase} had similar levels of basal and DNA damage–activated acetyltransferase activity as the wild-type p400 (Fig. 6 c). The p400^{ATPase} mutant is therefore recruited to DSBs (Fig. 6 a) and the Tip60 associated with the p400^{ATPase} mutant remains responsive to DNA damage (Fig. 6 c). However, the levels of histone H4 acetylation were slightly reduced in cells expressing the p400^{ATPase} mutant (Fig. 6 b), suggesting that p400's ATPase activity is required for efficient acetylation of histone H4 at DSBs. This could occur, for example, through p400-mediated changes in chromatin structure that facilitate Tip60 acetylation of histone H4. In conclusion, Fig. 6 demonstrates that recruitment of p400 to DSBs

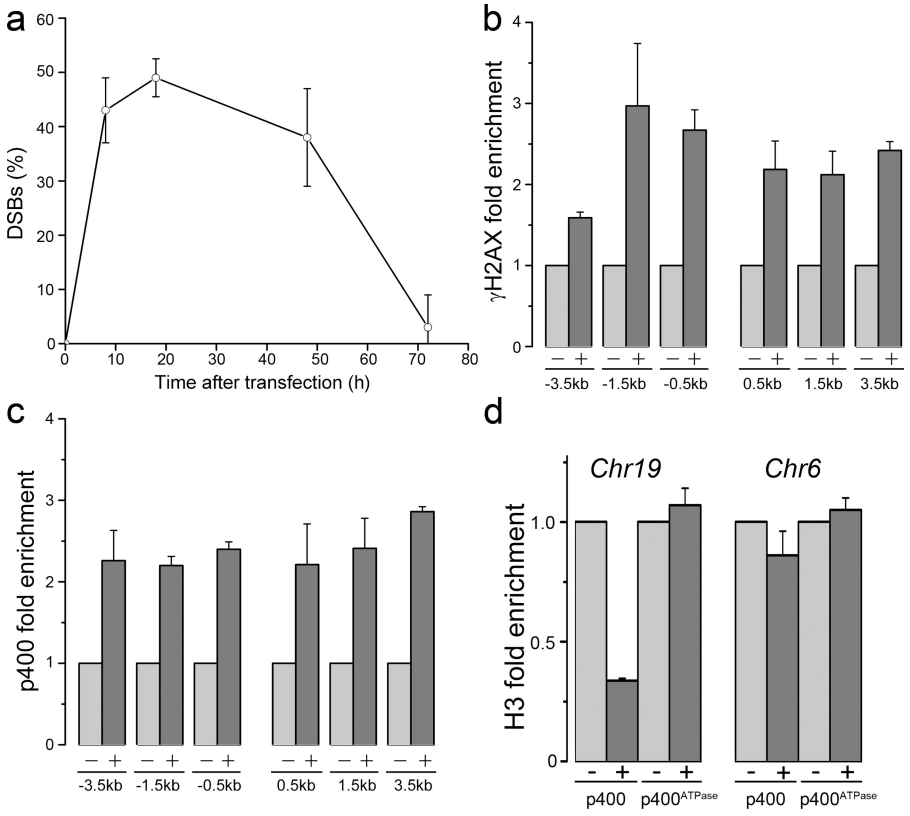

Figure 5. **p400 is recruited to DSBs generated by the p84-ZFN.** (a) 293T cells were transiently transfected with p84-ZFN, DNA extracted and examined by qPCR to monitor the fraction of cells with DSBs. (b) 293T cells were transiently transfected with vector (−) or p84-ZFN (+). 18 h later, cells were processed for ChIP analysis using anti–γ-H2AX antibody and primer pairs located left and right of the DSB. ChIP data points were calculated as IP DNA/input DNA (see Materials and methods). Fold enrichment is the relative fold increase in signal from the ZFN samples compared with the vector samples, which were normalized to give a value of 1. Results ± SE (n = 3). (c) 293T cells were transiently transfected with vector (−) or p84-ZFN (+) as described in b. Cells were processed for ChIP analysis using anti-p400 antibody. Results ± SE (n = 3). (d) 293T cells expressing p400 or p400^{ATPase} were transiently transfected with vector (−) or p84-ZFN (+). 18 h later, cells were preextracted in 1.0 M NaCl to release histones, and the nuclear pellet collected and processed for ChIP analysis as described in Materials and methods. Samples were immunoprecipitated with anti-H3 antibody. qPCR was performed using primers located at +1.5 kb relative to the ZFN site on chromosome 19 (*Chr19*), or at nucleotide positions 122,788,208 and 122,788,440 on chromosome 6 (*Chr 6*). Results ± SE (n = 3).

is independent of the ATPase activity of p400, indicating that the failure to detect decreased nucleosome stability in p400^{ATPase} cells is due to the loss of the intrinsic ATPase activity of p400.

Tip60 can also acetylate lysine 5 of H2AX (Jha et al., 2008), and may regulate the turnover of the *Drosophila* H2A.Z homologue, H2Av, at DSBs (Kusch et al., 2004). However, mutation of lysine 5, or all four potential lysine acetylation sites in the N-terminus of H2AX (Fig. S4 a), had minimal impact on the p400-dependent decrease in nucleosome stability. Acetylation of histones by Tip60 may therefore have distinct functions, with acetylation of H4 mediating the altered nucleosome stability observed here, and acetylation of H2AX contributing to turnover of γ-H2AX (Kusch et al., 2004; Ikura et al., 2007).

γ-H2AX plays a key role in recruiting DNA damage response proteins at DSBs, suggesting that γ-H2AX may recruit p400 to DSB. MEFs derived from H2AX$^{-/-}$ mice expressing either vector (H2AX$^{-/-}$) or complemented with wild-type H2AX (H2AX^{wt}) were exposed to bleomycin (Fig. 7 a). H2AX^{wt} cells exhibited decreased nucleosome stability after bleomycin exposure (Fig. 7 a), whereas H2AX$^{-/-}$ cells displayed no significant decrease in nucleosome stability. Although γ-H2AX is required to decrease nucleosome stability, ATM, which directly phosphorylates H2AX, was not required (Fig. 1). This is due to the fact that H2AX can be phosphorylated by both the ATM and DNA-PKcs kinases, so that loss of ATM activity does not significantly impair the formation of γ-H2AX domains (Stiff et al., 2004). In fact, when H2AX^{wt} MEFs were treated with the dual specificity ATM/DNA-PKcs inhibitor wortmannin (which inhibits phosphorylation of H2AX; Fig. S4 b; Stiff et al., 2004), the decrease in nucleosome stability caused by bleomycin was inhibited. Phosphorylation of H2AX is therefore required for p400-dependent alterations in nucleosome stability.

γ-H2AX recruits mdc1 to DSBs, which then serves as a platform to concentrate DNA repair proteins at sites of DNA damage (Spycher et al., 2008). To determine if mdc1 was required to recruit p400 to DSBs, mdc1 was silenced by shRNA (Fig. S4, c and d). Silencing of mdc1 blocked the p400-dependent decrease in nucleosome stability (Fig. 7 b). Similar results were seen with mdc1$^{-/-}$ MEFs (Fig. S4 e). These results imply that recruitment of mdc1 to γ-H2AX is required to position p400 at DSBs. Immunoprecipitation of p400 demonstrated that p400 and mdc1 were present as a preformed complex and that the p400–mdc1 complex was not altered by DNA damage (Fig. S4 f), consistent with reports that mdc1 forms stable complexes with several DNA damage response proteins (Melander et al., 2008; Spycher et al., 2008). In addition, ChIP assays (Fig. 7 c) demonstrate that p400 is not recruited to ZFN-generated DSBs in the absence of mdc1. Together, the immunoprecipitation (Fig. S4 f) and ChIP data (Fig. 7 c) are consistent with a model in which p400 is recruited to DSBs through interaction between mdc1 and γ-H2AX. The p400-dependent decrease in nucleosome stability therefore occurs after phosphorylation of H2AX and assembly of mdc1 onto the chromatin.

DNA damage leads to increased ubiquitination of the chromatin by the RNF8 ubiquitin ligase (Huen et al., 2007; Kolas et al., 2007; Mailand et al., 2007). To determine if this ubiquitination contributes to decreased nucleosome stability, RNF8 was targeted using both siRNA (Fig. S4 h) and by overexpressing an HA-RNF8 protein lacking the ring domain (Huen et al., 2007; Fig. 7 d and Fig. S4 g). In both cases (Fig. 7 d and Fig. S4 h),

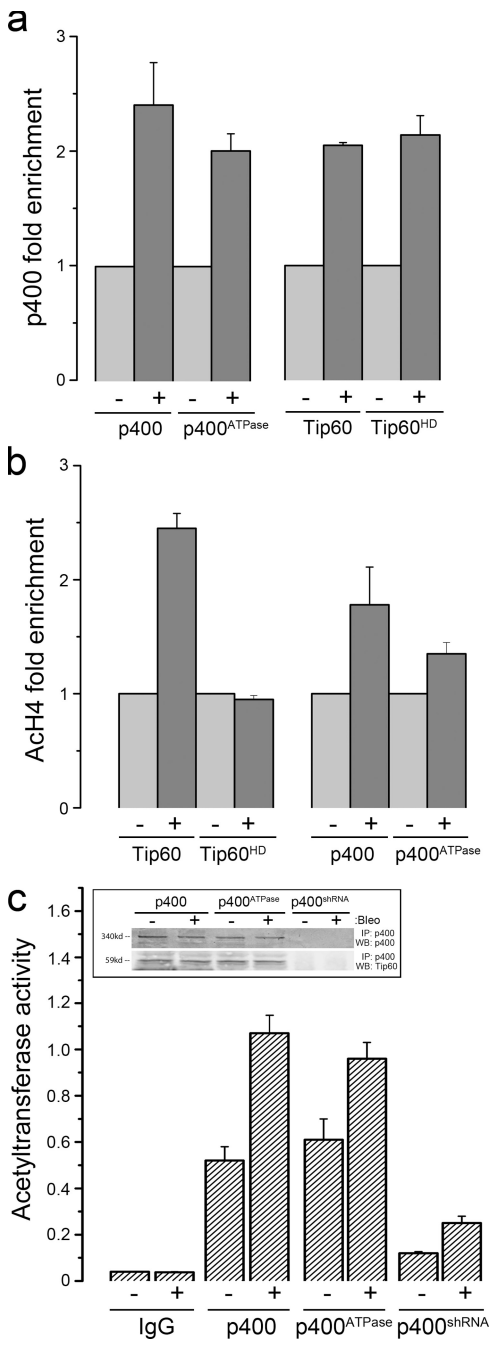

Figure 6. **Acetylation of histone H4 by the p400–Tip60 complex.** (a) 293T cells expressing wild-type Tip60 (Tip60^{wt}), catalytically inactive Tip60 (Tip60^{HD}), wild-type p400 (p400), or p400 lacking ATPase activity (p400^{ATPase}) were transiently transfected with vector (−) or p84-ZFN (+), and ChIP assays using anti-p400 antibody performed using primers located at +1.5 kb relative to the DSB. Results ± SE (n = 3). (b) 293T cells expressing Tip60^{wt}, Tip60^{HD}, p400, or p400^{ATPase} were transiently transfected with vector (−) or p84-ZFN (+). 18 h later, ChIP assays were performed using anti-acetylH4 antibody (AcH4) and primers located +1.5 kb relative to the DSB. Results ± SE (n = 3). (c) p400 was immunopurified from 293T cells expressing either HA-p400, HA-p400^{ATPase}, or cells in which p400 was silenced with shRNA and the associated Tip60 acetyltransferase activity measured. Cells were exposed to bleomycin (+: 5 μM for 40 min) where indicated. Inset: Immunoprecipitates were separated by SDS-PAGE, and p400 and coprecipitating Tip60 detected by Western blot.

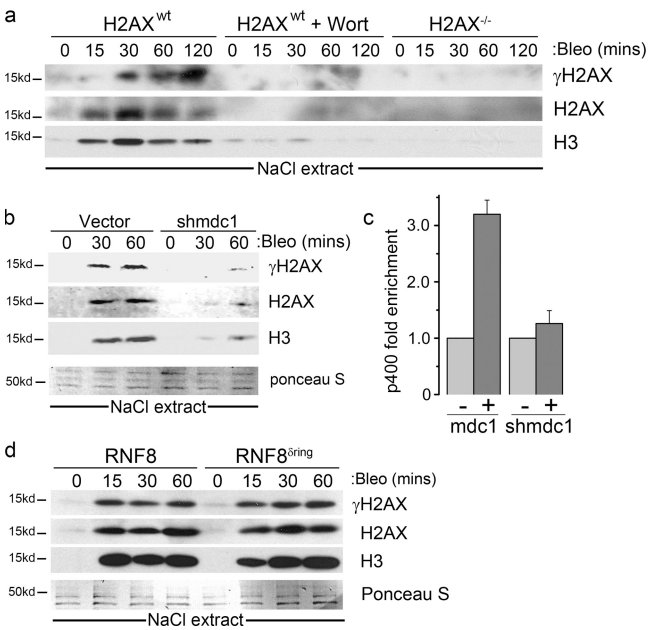

Figure 7. **Recruitment of p400 to DSBs requires mdc1.** (a) H2AX$^{-/-}$ MEFs or H2AX$^{-/-}$ MEFs complemented with H2AX (H2AX^{wt}) were exposed to 5 μM bleomycin. 20 μM Wortmannin was added 60 min before bleomycin. Cells were fractionated in 1.0 M NaCl, and released histones detected by Western blot. (b) 293T cells expressing vector or mdc1 shRNA (shmdc1) were exposed to 5 μM bleomycin. Cells were fractionated in 1.0 M NaCl, and released histones detected by Western blot. (c) 293T cells expressing GFP or mdc1 shRNA were transiently transfected with vector or p84-ZFN. 18 h later, ChIP assays using p400 antibody and primer pairs located at +1.5 kb were performed. Results ± SE (n = 3). (d) 293T cells stably expressing FLAG-RNF8 or RNF8 lacking the catalytic domain (FLAG-RNF8$^{\delta ring}$), which functions as a dominant-negative inhibitor of endogenous RNF8 function (Huen et al., 2007), were exposed to bleomycin. Cells were fractionated in 1.0 M NaCl, and released histones detected by Western blot.

suppression of RNF8 did not affect the p400-dependent decrease in nucleosome stability, indicating that RNF8-dependent ubiquitination of chromatin does not contribute to the p400-dependent decrease in nucleosome stability.

Because p400 functions at a relatively late stage in the DNA damage signaling process, we determined if the recruitment of late components of the DNA damage response, including 53BP1 and brca1, required p400. Consistent with previous reports (Huen et al., 2007; Mailand et al., 2007), recruitment of brca1 to DSBs was not detected until 15–30 min after exposure to IR (Fig. 8 a). Strikingly, no significant accumulation of brca1 was detected in cells expressing the p400^{ATPase} mutant (Fig. 8, a and c), although formation of γ-H2AX foci was normal (Fig. 8 c). Similarly, the recruitment of 53BP1 to DSBs was significantly impaired at early times in p400^{ATPase} cells, although 53BP1 eventually accumulated to near-normal levels by 60 min in the p400^{ATPase} cells (Fig. 8 b). The recruitment of both brca1 and 53BP1 to DSBs is therefore dependent on p400, and is consistent with previous reports that another component of NuA4, Trrap, is required for brca1 and 53BP1 accumulation at DSBs (Murr et al., 2006). The recruitment of brca1 to DSBs also requires recruitment of the RNF8 ubiquitin ligase, which ubiquitinates chromatin-associated proteins and facilitates the recruitment of RAP80 and the ccdc98–brca1 complex to DSBs (Huen et al., 2007;

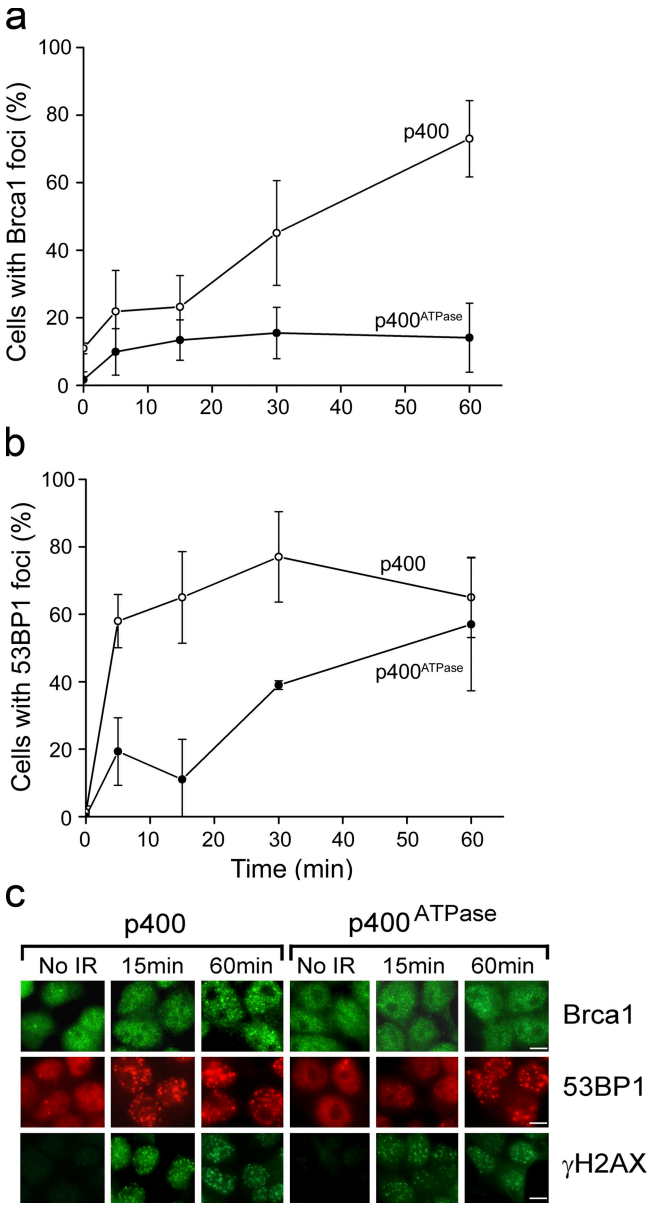

Figure 8. **p400 is required to recruit 53BP1 and brca1 to DSBs.** 293T cells expressing p400 or p400^{ATPase} were irradiated (2Gy). At the indicated times, cells were fixed and processed by immunofluorescent staining to detect either brca1 (a) or 53BP1 (b) foci. Cells with >5 foci were counted, with an average of 100 cells per slide. Experiments represent at least three independent replicates. Results ± SE (n = 100). (c) 293T cells expressing p400 or p400^{ATPase} were irradiated (2Gy). At the indicated times, cells were fixed and processed by immunofluorescent staining to detect brca1, 53BP1 foci, and γ-H2AX. Bar, 5 µm.

Kolas et al., 2007; Mailand et al., 2007). To determine if p400 regulates brca1 recruitment by modulating RNF8 function, we examined if p400 alters the ability of RNF8 to ubiquitinate its target proteins. RNF8-mediated ubiquitination can be detected using the FK2 antibody, which detects ubiquitin conjugated to proteins (Huen et al., 2007; Kolas et al., 2007; Mailand et al., 2007). FK2 foci were detected 15 min after exposure to IR, and remained elevated for at least 60 min, whereas cells expressing the p400^{ATPase} mutant had few FK2 at 60 min (Fig. 9, a and b). To further confirm this observation, ChIP analysis with the FK2 antibody revealed extensive ubiquitination of a large chromatin domain after DSB generation by the p84-ZFN (Fig. 9 c); formation of this domain was significantly impaired in cells expressing the p400^{ATPase} mutant. Fig. 9 clearly demonstrates that p400 is required for the RNF8-dependent ubiquitination of chromatin adjacent to DSBs. The failure to detect significant accumulation of brca1 in cells expressing the p400^{ATPase} mutant (Fig. 8 a) therefore reflects the inability of the p400^{ATPase} mutant cells to ubiquitinate the chromatin, which is required to localize the rap80–brca1 complex onto the chromatin (Huen et al., 2007; Kolas et al., 2007; Mailand et al., 2007). This implies that p400-dependent changes in nucleosome stability are required either to recruit RNF8 to DSBs, or to facilitate the ubiquitination of chromatin target proteins by RNF8 at DSBs. Fig. 9, d and e demonstrate that RNF8 was efficiently recruited to DSBs in both normal and p400^{ATPase} cells, although the formation of FK2 foci was significantly impaired in the p400^{ATPase} cells. Overall, the results demonstrate that p400's ATPase activity is required to facilitate the ubiquitination of chromatin target proteins by RNF8 adjacent to DSBs. The failure to recruit brca1 to DSBs in p400^{ATPase} cells therefore reflects the failure of RNF8 to ubiquitinate the chromatin and to create binding sites for the rap80–brca1 complex.

Discussion

Here, we reveal that DSBs lead to the formation of chromatin domains in which the histone–DNA interaction within nucleosomes is weakened. However, the nucleosomes remain an integral part of the chromatin, indicating that the decrease in histone–DNA interaction reflects a switch in chromatin conformation to a more open, flexible structure after DNA damage. The p400-dependent decrease in nucleosome stability observed here was preferentially located within the γ-H2AX domains that form adjacent to DSBs (Bonner et al., 2008). This conclusion is supported by several lines of evidence. First, the histones released from the chromatin by NaCl fractionation are enriched for γ-H2AX relative to other histones, indicating that they are preferentially derived from the γ-H2AX domains adjacent to the DSB. Second, ChIP assays indicate that NaCl fractionation removed histone H3 from regions adjacent to the ZFN-generated DSBs. Third, both Tip60 and p400 are localized to the chromatin adjacent to the DSB. Collectively, these results imply that the p400-mediated decrease in nucleosome stability is preferentially focused within chromatin domains contiguous with the DSB. Previous work has shown that DNA damage can alter chromatin architecture by two distinct pathways—an ATM-independent pathway that alters local chromatin structure (Shroff et al., 2004; Tsukuda et al., 2005; Kruhlak et al., 2006) and an ATM/phospho-kap1–dependent pathway that initiates global chromatin relaxation, including heterochromatin (Ziv et al., 2006; Goodarzi et al., 2008). However, the p400-mediated decrease in nucleosome stability did not require either ATM or kap1 phosphorylation, indicating that it is distinct from the phospho-kap1/ATM–mediated pathway of global decompaction previously described (Ziv et al., 2006). Our results are therefore more consistent with a previous report that chromatin structural changes at DSBs are independent of ATM (Kruhlak et al., 2006). p400 is

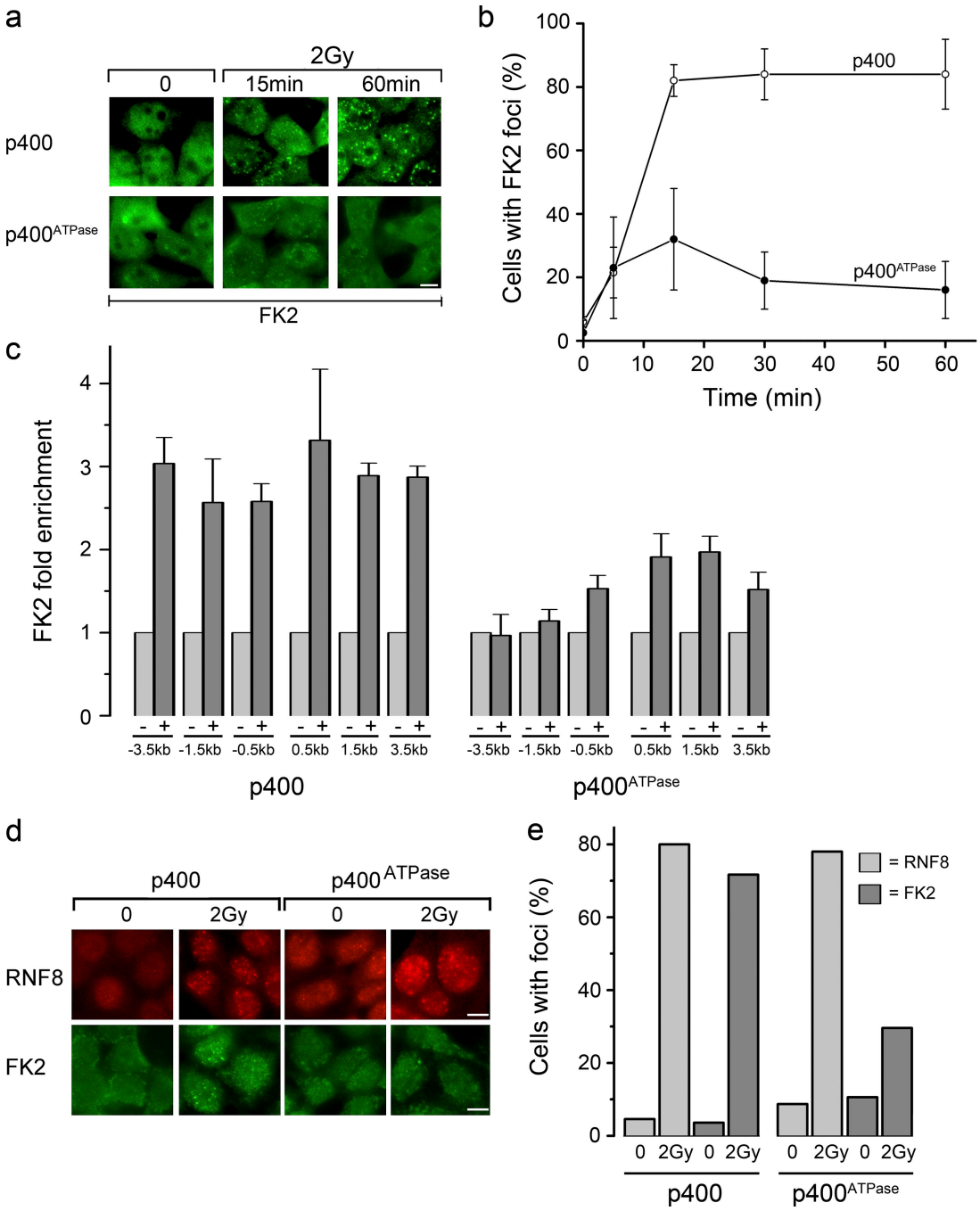

Figure 9. **p400 is required for RNF8-dependent ubiquitination of the chromatin.** (a) 293T cells expressing p400 or p400^{ATPase} were irradiated as indicated. Cells were fixed and processed by immunofluorescent staining using FK2 antibody. Bar, 5 μm. (b) 293T cells expressing p400 or p400^{ATPase} were irradiated (2Gy). Immunofluorescent staining using the FK2 antibody was used to detect proteins ubiquitinated by RNF8. Cells with >5 foci per cell were counted, with an average of 100 cells per slide. Results ± SE (n = 100). (c) 293T cells expressing p400 or p400^{ATPase} were transiently transfected with vector or p84-ZFN. 18 h later, ChIP assays using the FK2 antibody and primer pairs located at −3.5 kb, −1.5 kb, −0.5 kb, 0.5 kb, 1.5 kb, and 3.5 kb were performed. Results ± SE (n = 3). (d) 293T cells expressing p400 or p400^{ATPase} were irradiated (2Gy), fixed, and immunofluorescent staining to detect RNF8 and FK2 performed. Bar, 5 μm. (e) Quantitation of FK2 and RNF8 foci in p400 and p400^{ATPase} cells from d. Cells with >5 foci were counted, with an average of 100 cells per slide counted. Experiments represent at least three independent replicates. Results ± SE (n = 100).

therefore likely to function primarily within the chromatin domains adjacent to the DSB, where it functions to destabilize nucleosome structures. However, our results do not exclude the possibility that a fraction of the histones removed by NaCl treatment are derived from regions that are remote from the DSB, or even on adjacent chromosomes. Whether this reflects p400-dependent remodeling at sites far from the DSB, or is a consequence of chromatin changes at the DSB that propagate across the entire chromatin is not currently known.

Several lines of evidence suggest that p400, Trrap, and Tip60 function together as components of the NuA4 complex to alter nucleosome stability during DSB repair. First, although p400,

Tip60, and Trrap can function individually in the cell, they are only found together as components of NuA4 (Doyon and Côté, 2004; Doyon et al., 2004). Second, yeast NuA4 is recruited to DSBs (Downs et al., 2004). Third, the acetyltransferase activity of the p400 complex was increased by DNA damage, indicating a functional interaction between p400 and Tip60 during DSB repair. Collectively, we propose that p400, Trrap, and Tip60 are recruited to DSBs as components of the NuA4 complex. This would then focus the catalytic activities of p400 and Tip60 onto spatially confined regions of chromatin, allowing them to alter the local nucleosome architecture.

Significant insight into how p400's ATPase activity and Tip60's acetyltransferase activity co-coordinately regulate nucleosome stability was obtained. Tip60 acetylates H4 (Bird et al., 2002; Downs et al., 2004; Doyon et al., 2004; Murr et al., 2006) and H2AX (Kusch et al., 2004; Jha et al., 2008) after DNA damage. However, the p400-dependent decrease in nucleosome stability did not require acetylation of H2AX by Tip60 (Kusch et al., 2004; Jha et al., 2008). Instead, the decreased nucleosome stability was associated with increased acetylation of histone H4 at DSBs by Tip60. Histone acetylation may alter nucleosome structure through at least 2 mechanisms—charge neutralization and the recruitment of chromatin-modifying proteins (Choi and Howe, 2009). Acetylation of the N terminus of histone H4 can induce small changes in nucleosome structure (Tóth et al., 2006; Ferreira et al., 2007), potentially weakening the DNA–histone interaction (Wang and Hayes, 2008). Further, acetylation of H4 on lysine 16 (Dion et al., 2005; Shogren-Knaak et al., 2006), a site acetylated by Tip60 (Bird et al., 2002; Doyon et al., 2004), specifically inhibits nucleosome packing. The ability of Tip60 to acetylate H4 at DSBs may reduce both the stability of the histone–DNA interaction within nucleosomes and facilitate the unpacking of higher order nucleosome arrays (Kusch et al., 2004; Brower-Toland et al., 2005; Murr et al., 2006; Shogren-Knaak et al., 2006). This process also required the ATPase activity of the p400 motor protein (Doyon et al., 2004). p400 has histone exchange activity, including the ability to exchange H2A.Z (Fuchs et al., 2001; Kusch et al., 2004; Gévry et al., 2007), but does not function to evict nucleosomes from the chromatin. The decrease in nucleosome stability after DNA damage therefore reflects increased acetylation of histones, including H4, by Tip60, which promotes both unpacking of higher order nucleosome arrays by p400 as well as reducing the strength of histone–DNA interactions within nucleosomes. p400 and Tip60 therefore function together to alter chromatin structure and facilitate repair of DSBs.

The p400-mediated alterations in chromatin structure were essential to recruit brca1 and 53BP1 to DSBs. This is consistent with a previous report that Trrap is also required to locate brca1 and 53BP1 to DSBs (Murr et al., 2006). Recruitment of brca1 to DSBs also involves the RNF8 (and RNF168) ubiquitin ligases, which ubiquitinate histones and other chromatin targets at DSBs (Huen et al., 2007; Kolas et al., 2007; Mailand et al., 2007; Doil et al., 2009). This ubiquitination creates a binding site for the ubiquitin-interacting domain of RAP80, facilitating the recruitment of the RAP80–abraxas–brca1 complex to DSBs. In the absence of the p400-mediated decrease in nucleosome stability, RNF8-dependent ubiquitination and recruitment of brca1 to DSBs was abolished. This clearly demonstrates that the decreased nucleosome stability and associated changes in chromatin architecture caused by p400 are required for RNF8 to access and ubiquitinate the chromatin-associated proteins, and to promote recruitment of brca1 to DSBs.

Although p400 was essential to recruit brca1 to DSBs, loss of p400 delayed (but did not abolish) the accumulation of 53BP1 at DSBs, indicating multiple pathways for recruitment of 53BP1 to damaged chromatin. Although RNF8 plays a key role in recruiting 53BP1 to DSBs (Huen et al., 2007; Kolas et al., 2007; Mailand et al., 2007), the positioning of 53BP1 at DSBs may also involve direct binding of 53BP1 to H4K20me2 (Sanders et al., 2004; Botuyan et al., 2006). The p400-mediated decrease in nucleosome stability may therefore facilitate both ubiquitination (and potentially sumoylation; Galanty et al., 2009; Morris et al., 2009) of the chromatin, as well as exposing buried H4K20me2 sites that facilitate the recruitment of 53BP1 to DSBs. Although RNF8 ubiquitinates H2A and other proteins (Huen et al., 2007; Kolas et al., 2007; Mailand et al., 2007; Doil et al., 2009; Stewart et al., 2009), the exact target for RNF8 on the chromatin is not clear. p400-mediated changes in nucleosome structure may therefore also function to recruit (or evict) proteins from the chromatin, including novel proteins that are targets for either ubiquitination or sumoylation.

The key role for p400 in altering nucleosome stability at DSBs predicts a central role for p400 in DNA repair. In fact, $p400^{ATPase}$ cells exhibited both increased sensitivity to IR and increased accumulation of chromosome aberrations. This is consistent with previous reports indicating that the p400/Tip60 ratio plays a key role in restraining proliferation of tumor cells, and that deregulation of this balance in colorectal cancer cells contributes to loss of the oncogene-induced DNA damage response (Mattera et al., 2009). p400 therefore represents a new class of DNA damage response proteins involved in regulating chromatin structure at DSBs and in facilitating efficient DSB repair.

The results suggest the following model. Detection of DSBs leads to the phosphorylation of H2AX and deposition of mdc1 onto the chromatin. Subsequently, p400, Trrap, and Tip60 are recruited to mdc1, most likely as subunits of the NuA4 complex. p400's ATPase activity then disrupts the local histone–DNA interactions, altering the nucleosome architecture and facilitating the hyperacetylation of H4 by Tip60. This results in destabilization of the nucleosomes, and promotes unpacking of stacked nucleosome arrays. The overall result is to shift the local chromatin structure into a relaxed, more open conformation. Further, these regions of decreased nucleosome stability were preferentially located in regions of high γ-H2AX density, suggesting that γ-H2AX focal regions surrounding DSBs represent relaxed, open chromatin domains. These open chromatin structures then expose RNF8 ubiquitination substrates on the chromatin (Huen et al., 2007; Kolas et al., 2007; Mailand et al., 2007) as well as exposing cryptic histone methylation sites, such as H4K20me2 (Sanders et al., 2004), which leads to recruitment of the brca1 and 53BP1 proteins to the DSB. The overall outcome is to facilitate DNA repair by increasing the mobility of the nucleosomes adjacent to the DSBs, promoting the post-translational modification of histones, and directing the recruitment and retention of protein factors at DSBs.

In conclusion, we provide the first direct evidence for altered nucleosome stability at DSBs, and have identified key players in this process—p400, Trrap, and Tip60. Further, these results demonstrate that changes in nucleosome stability at DSBs can regulate both ubiquitination of chromatin by RNF8 and potentially modulate access to histone modifications, such as histone methylation, which are buried within the packed nucleosome arrays that constitute chromatin fibers. Finally, these results identify p400 as a novel DNA damage response protein that is critical in facilitating the accumulation of the brca1 protein at sites of DNA damage.

Materials and methods

Cell culture, plasmids, and transfection

293T cells were maintained in DME supplemented with 10% fetal bovine serum. $Tip60^{wt}$ and $Tip60^{HD}$ cells, shp400 cells, shTrrap cells, and $HCT116^{shRad50}$ cells were maintained as described previously (Chan et al., 2005; Sun et al., 2005; Zhong et al., 2005). GM5849 A-T cells complemented by expression of ATM are described in Sun et al. (2005, 2009). $H2AX^{-/-}$ MEFs cells were maintained in DME supplemented with 15% fetal bovine serum, 0.8 mM β-mercaptoethanol, and 1% L-glutamine. Cells were irradiated using a Cs^{137} irradiator and clonogenic cell survival monitored as in Sun et al. (2005). Averages were calculated from three independent plates, and expressed plus or minus the standard deviation (SD). To measure chromosome aberrations, HeLaS3 cells were irradiated (2Gy) and allowed to recover for 14 h. Colcemid was added, and metaphase spreads prepared as described in Yang et al. (2001). Metaphase spreads (at least 50) were scored manually under the microscope for aberrations, with the observer blinded to the experimental conditions. Statistical analysis was performed using the Analysis ToolPak program of Microsoft Excel to establish statistical significance.

The $p400^{ATPase}$ mutant was constructed using pCMV-Flag-EP400 (obtained from Chan et al., 2005) and the primer pairs: 5′-GATGAAGCTGGGCTGGGTGCAACAGTGCAGATCATTGC-3′; 5′-GCAATGATCTGCACTGTTGCACCCAGCCCAGCTTCATC-3′, which introduces the mutation K1085L into the ATPase domain of p400 (the p400 sequence can be found at GenBank/EMBL/DDBJ under accession no. NP_056224). Mutagenesis of p400 and H2AX was performed using the QuikChange Site-Directed Mutagenesis kit (Agilent Technologies). 293T, HeLa, and MEF cells were transfected using Lipofectamine 2000 according to the manufacturer's instructions (Invitrogen), and selected using puromycin. H2AX was inserted into plasmid pIRESpuro3 (Takara Bio Inc.), and wild-type H2AX ($H2AX^{wt}$), H2AX with an alanine mutation at lysine 5 ($H2AX^{K5A}$), or H2AX with all four N-terminal lysine residues mutated to arginine ($H2AX^{K->R}$) expressed in $H2AX^{-/-}$ MEFs. 293T lentiviral mdc1 shRNA clones and GFP control shRNA were obtained from The RNAi Consortium (Broad Institute, Cambridge, MA). Plasmids were packaged with VSV-G expressing constructs phCMV-G and PCMVδ8.2 plasmid and transfected into 293T cells using Lipofectamine 2000. After 48 h, viral particles were harvested from the culture medium and used to prepare stable cell lines expressing GFP or mdc1 shRNA after selection with puromycin. siRNAs targeting RNF8 (#1: 5′-UUCUCCUUGGGCUAUCUCCAAACCC-3′; and #2: 5′-GGAGAAUGCGGAGUAUGAAUAUGAA-3′) were transiently transfected into 293T cells using Lipofectamine 2000 (Invitrogen) as described previously by us (Sun et al., 2005). The p84-ZFN vector AAVS1 was transfected into cells using Lipofectamine 2000.

Cell lysates, immunoprecipitation, and Western blot analysis

Antibodies used: p400 (Bethyl Laboratories, Inc.); H2AX, 53BP1 (Cell Signaling Technology); γ-H2AX, Tip60, FK2, H2B, acetylated H4 (Millipore); H3, H4, RNF8 (Abcam); ATM, PC116, brca1 (EMD); ATM2C1 (GeneTex); pS1981-ATM (R&D Systems); RNF8 antibody for foci experiment was a generous gift from Junjie Chen (MD Anderson Cancer Center, University of Texas, Houston, TX). To extract total histones, cells were resuspended in 500 µl buffer A (20 mM Hepes, pH 7.9, 0.5 mM DTT, 1 mM PMSF, 1.5 mM $MgCl_2$, and 0.1% Triton) containing 0.4 M NaCl and centrifuged at 12,000 *g* for 5 min. The pellet was resuspended in buffer B (10 mM Hepes, pH 7.9, 10 mM KCl, 1.5 mM $MgCl_2$, 0.5 mM DTT, and 1 mM PMSF) and 2.0N sulfuric acid added to a final concentration of 0.4N. Samples were cleared by centrifugation (12,000 *g*) and histones precipitated with 20% trichloroacetic acid for 30 min. Histones were collected by centrifugation (12,000 *g* for 15 min), washed once in acetone, and resuspended in 10 mM Hepes, pH 7.9. For immunoprecipitation, 4×10^6 cells were resuspended in 1 ml NETN buffer (50 mM Tris, pH 7.5, 150 mM NaCl, 1 mM EDTA, 1% NP-40, 1 mM DTT, and 1 mM PMSF) for 30 min, followed by centrifugation at 13,000 *g* for 15 min. The supernatant was precleared with Protein A/G plus beads (Santa Cruz Biotechnology, Inc.) at 4°C for 30 min. 1–5 µg antibody and 30 µl Protein A/G plus beads (Santa Cruz Biotechnology, Inc.) were added, incubated for 3 h, washed four times in NETN buffer containing 0.5% NP-40, and bound proteins eluted in SDS sample buffer. For Western blots, equal amounts of protein (determined using the DC Protein Assay kit; Bio-Rad Laboratories) were separated by SDS-PAGE and transferred to PVDF membranes. Membranes were blocked with 5% nonfat dry milk, incubated with primary antibodies for 1 h, and washed in TBST (20 mM Tris, pH 7.5, 137 mM NaCl, and 0.1% Tween 20) followed by goat anti–mouse IR Dye-800CW– or goat anti–rabbit IR Dye-680CW–conjugated secondary antibodies (Li-Cor Inc.). Imaging was performed using the Li-Cor Odyssey Near Infra Red System, and analyzed using the Odyssey software system 3.0 package (Li-Cor Inc.).

For HAT assays, cells were lysed in buffer C (20 mM Hepes, pH 7.5, 150 mM NaCl, 0.2% Tween 20, 1.5 mM $MgCl_2$, 1 mM EDTA, 2 mM DTT, 50 mM NaF, 500 µM Na_3VO_4, and 1 mM PMSF) and cleared lysates were immunoprecipitated with p400 antibody (Bethyl Laboratories, Inc.). Immunoprecipitates were washed twice in HAT assay buffer (50 mM Tris, pH 8, 10% glycerol, 0.1 mM EDTA, and 1 mM DTT) and incubated in 60 µl of HAT assay buffer containing 100 µM acetylCoA and 0.5 µg biotinylated histone H4 peptide for 30 min at 30°C. An aliquot of the reaction was immobilized onto streptavidin plates and acetylation detected by ELISA as described previously by us (Sun et al., 2005, 2007).

Nucleosome stability assay

Cells were harvested and washed twice in ice-cold PBS by centrifugation at 1,000 rpm. Cell pellet was resuspended completely in 500 µl buffer A (20 mM Hepes, pH 7.9, 0.5 mM DTT, 1 mM PMSF, 1.5 mM $MgCl_2$, and 0.1% Triton) containing 1.0 M NaCl. Cells were incubated for 40 min at 4°C with constant agitation. Samples were then centrifuged at 100,000 *g* (Ultracentrifuge; Beckman Coulter) for 20 min, and the supernatant, containing released histones, retained for further analysis. In some experiments, cells were first incubated in buffer A with 0.15 NaCl to remove cell membrane and cytosolic contents. The nuclear fraction was then collected by centrifugation and the nuclear pellet resuspended in buffer A plus 1.0 M NaCl and processed as described above. Essentially identical results were obtained using both methods.

Quantitation of H2AX and γ-H2AX levels

To calculate the relative levels of H2AX and γ-H2AX in the NaCl extracts, serial dilutions of total histones were separated by SDS-PAGE. Western blot analysis was then performed using H2AX and γ-H2AX primary antibodies followed by goat anti–mouse IR Dye-800CW– or goat anti–rabbit IR Dye-680CW–conjugated secondary antibodies. Infrared signals were scanned into the Li-Cor Odyssey Near Infra Red System, and the Li-Cor software package used to establish linear ranges for signal detection of H2AX and γ-H2AX. Calibration curves are shown in Fig. S1 a, and were used to determine the relative ratio of γ-H2AX/H2AX in both the total cell extracts and in the NaCl extract.

ChIP assays

Chromatin immunoprecipitation (ChIP) assays used the SimpleChIP Enzymatic Chromatin IP kit (Cell Signaling Technology). In brief, cells were fixed in 1% methanol-free formaldehyde for 10 min and glycine added to block the reaction. Cells were washed twice in PBS, lyzed in ChIP buffer (Cell Signaling Technology), and sonicated (Sonic 250; Thermo Fisher Scientific) to generate DNA fragments with lengths between 200 and 1,000 bp. Insoluble debris was removed by centrifugation. A portion of each supernatant was diluted in ChIP elution buffer and digested with proteinase K at 65°C for 2 h and the released DNA fragments isolated by spin columns. The DNA was quantitated by RT-PCR using primers (listed below) to GAPDH (Input DNA). The remaining supernatant was diluted in ChIP buffer and equivalent amounts of input DNA incubated with primary antibody (2 h at 4°C) followed by collection of immune complexes on protein G–Agarose beads precoated with sperm DNA. Immune complexes were washed in low and high salt ChIP buffer (Cell Signaling Technology), the protein–DNA complex eluted, and the DNA–protein cross-links reversed by addition of NaCl and heating at 65°C for 2 h. After proteinase K digestion, DNA was purified using the spin column and then quantitated by qPCR using a DNA Engine Real-Time PCR machine (Bio-Rad Laboratories).

PCR amplification protocol: 95°C for 5 min; followed by 33 cycles of 95°C for 30 s; 55°C for 30 s; 72°C for 30 s followed by 72°C for 5 min. Serial dilutions of the starting material were used to determine the linear

range of PCR amplification rate before choosing the volume of extracted DNA used in the reaction. GAPDH was used to standardize amounts of input DNA for each reaction. Standard controls included immunoprecipitation with IgG and qPCR of immunoprecipitated DNA with GAPDH, both of which yielded essentially no signal. Relative folds of enrichment were optimized by the input control and expressed as IP/Input DNA. The relative increase in signal after cutting by the p84-ZFN was calculated as $[IP^{ZFN}/Input^{ZFN}]/[IP^{Control}/Input^{Control}]$. All ChIP assays were repeated at least twice, and individual qPCR reactions were performed in triplicate, with results presented ±SD. PCR primers: −0.5 kb (5′-TGGGTTCCCTTTTCCTTCTC-3′ and 5′-GTCCAGGCAAAGAAAGCAAG-3′); +0.5 kb (5′-ATGGTGCGTCCTAGGTGTTC-3′ and 5′-CCAAGGACTCAAACCCAGAA-3′); −1.5 kb (5′-GGGGCAGTCTGCTATTCATC-3′ and 5′-CGATGCACACTGGGAAGTC-3′); +1.5 kb (5′-CCTCAGCTCCAGTTCAGGTC-3′ and 5′-GGCTGTCACACTCCAGTTCA-3′); −3.5 kb (5′-CCGAGATCACATCACTGCAC-3′ and 5′-GGAAAGAGGAGGGAAGAGGA-3′); +3.5 kb (5′-TCGCCAGTGCTTTTTCTTTT-3′ and 5′-GTTGGGGGATGATGAAAATG-3′); GAPDH primers: (5′-CCTGACCTGCCGTCTAGAAAA-3′ and 5′-CTCCGACGCCTGCTTCAC-3′); DSB primers: (5′-CGGTTAATGTGGCTCTGGTT-3′ and 5′-ACAGGAGGTGGGGGTTAGAC-3′); Chr 6 primers: (5′-CATGGTCGTCAACCAAATGA-3′ and 5′-CCCAGAATCTTCTGACCTGCT-3′).

Immunofluorescence

Cells (on cover slides) were fixed in phosphate-buffered saline (PBS) containing 4% paraformaldehyde, blocked with 2% fetal bovine serum for 10 min, and permeabilized in 0.2% bovine serum albumin containing 0.2% saponin for 15 min. After a 1-h incubation with primary antibody, cells were washed three times with 0.2% Tween 20 and incubated for 1 h in secondary antibody (conjugated to either Texas red or FITC; Santa Cruz Biotechnology, Inc.). Slides were mounted with Fluoromount-G (SouthernBiotech) and imaged at room temperature. Images were collected with a microscope (AxioImager Z1; Carl Zeiss, Inc.) equipped with a color digital camera (Axiocam MRc Rev.3; Carl Zeiss, Inc.) and a Plan Apochromat oil M27 lens (63x, NA 1.4). Acquisition software and image processing used the AxioVision software package (Carl Zeiss, Inc.).

RT-PCR for mdc1 mRNA levels

Cells were lyzed in 1 ml Triazol and 200 µl chloroform, centrifuged, and the upper layer precipitated with isopropanol. Washed pellets were digested with DNase1, precipitated (3 M sodium acetate), and resuspended in water. 1 µg RNA and 50 ng random primers were heated to 70°C, chilled, and 1 µM dNTPs, 1 mM DTT, and 100 units of MMLV reverse transcription added to generate cDNA. RT-qPCR was performed using primers 5′-CTGGGTAGGTTCATCCTCCA-3′ and 5′-GGAAAGGGTGTCATTCTGGA-3′ and GAPDH primers as an internal control.

Online supplemental material

Fig. S1 demonstrates that the MRN complex and the ATM kinase are not required for reduced nucleosome stability. Fig. S2 demonstrates efficient silencing of p400 and Trrap expression, as well as expression of $p400^{ATPase}$ and $Tip60^{HD}$ in cells. Fig. S3 demonstrates that p84-ZFN generates DSBs in a range of cell lines, and activates the DNA damage response, including γ-H2AX production. Fig. S4 demonstrates that p400-mediated nucleosome stability requires both H2AX and mdc1, but does not require the ubiquitin ligase activity of RNF8. Online supplemental material is available at http://www.jcb.org/cgi/content/full/jcb.201001160/DC1.

We thank Junjie Chen for RNF8 constructs and antibodies, Ralph Scully for $mdc1^{-/-}$ MEFs, Homan Chan for p400 shRNA and Trrap shRNA cells, and Fyodor Urnov for the AAVS1.

This work was supported by grants from the National Cancer Institute (CA64585 and CA93602), the DOD Breast Cancer Program, and by a National Cancer Institute training grant to Y. Sun (T32 CA09078).

Submitted: 28 January 2010
Accepted: 1 September 2010

References

Bird, A.W., D.Y. Yu, M.G. Pray-Grant, Q. Qiu, K.E. Harmon, P.C. Megee, P.A. Grant, M.M. Smith, and M.F. Christman. 2002. Acetylation of histone H4 by Esa1 is required for DNA double-strand break repair. *Nature.* 419:411–415. doi:10.1038/nature01035

Bonner, W.M., C.E. Redon, J.S. Dickey, A.J. Nakamura, O.A. Sedelnikova, S. Solier, and Y. Pommier. 2008. GammaH2AX and cancer. *Nat. Rev. Cancer.* 8:957–967. doi:10.1038/nrc2523

Botuyan, M.V., J. Lee, I.M. Ward, J.E. Kim, J.R. Thompson, J. Chen, and G. Mer. 2006. Structural basis for the methylation state-specific recognition of histone H4-K20 by 53BP1 and Crb2 in DNA repair. *Cell.* 127:1361–1373. doi:10.1016/j.cell.2006.10.043

Brower-Toland, B., D.A. Wacker, R.M. Fulbright, J.T. Lis, W.L. Kraus, and M.D. Wang. 2005. Specific contributions of histone tails and their acetylation to the mechanical stability of nucleosomes. *J. Mol. Biol.* 346:135–146. doi:10.1016/j.jmb.2004.11.056

Brunet, E., D. Simsek, M. Tomishima, R. DeKelver, V.M. Choi, P. Gregory, F. Urnov, D.M. Weinstock, and M. Jasin. 2009. Chromosomal translocations induced at specified loci in human stem cells. *Proc. Natl. Acad. Sci. USA.* 106:10620–10625. doi:10.1073/pnas.0902076106

Cairns, B.R. 2005. Chromatin remodeling complexes: strength in diversity, precision through specialization. *Curr. Opin. Genet. Dev.* 15:185–190. doi:10.1016/j.gde.2005.01.003

Carrier, F., P.T. Georgel, P. Pourquier, M. Blake, H.U. Kontny, M.J. Antinore, M. Gariboldi, T.G. Myers, J.N. Weinstein, Y. Pommier, and A.J. Fornace Jr. 1999. Gadd45, a p53-responsive stress protein, modifies DNA accessibility on damaged chromatin. *Mol. Cell. Biol.* 19:1673–1685.

Chan, H.M., M. Narita, S.W. Lowe, and D.M. Livingston. 2005. The p400 E1A-associated protein is a novel component of the p53 --> p21 senescence pathway. *Genes Dev.* 19:196–201. doi:10.1101/gad.1280205

Choi, J.K., and L.J. Howe. 2009. Histone acetylation: truth of consequences? *Biochem. Cell Biol.* 87:139–150. doi:10.1139/O08-112

Dion, M.F., S.J. Altschuler, L.F. Wu, and O.J. Rando. 2005. Genomic characterization reveals a simple histone H4 acetylation code. *Proc. Natl. Acad. Sci. USA.* 102:5501–5506. doi:10.1073/pnas.0500136102

Doil, C., N. Mailand, S. Bekker-Jensen, P. Menard, D.H. Larsen, R. Pepperkok, J. Ellenberg, S. Panier, D. Durocher, J. Bartek, et al. 2009. RNF168 binds and amplifies ubiquitin conjugates on damaged chromosomes to allow accumulation of repair proteins. *Cell.* 136:435–446. doi:10.1016/j.cell.2008.12.041

Downs, J.A., S. Allard, O. Jobin-Robitaille, A. Javaheri, A. Auger, N. Bouchard, S.J. Kron, S.P. Jackson, and J. Côté. 2004. Binding of chromatin-modifying activities to phosphorylated histone H2A at DNA damage sites. *Mol. Cell.* 16:979–990. doi:10.1016/j.molcel.2004.12.003

Doyon, Y., and J. Côté. 2004. The highly conserved and multifunctional NuA4 HAT complex. *Curr. Opin. Genet. Dev.* 14:147–154. doi:10.1016/j.gde.2004.02.009

Doyon, Y., W. Selleck, W.S. Lane, S. Tan, and J. Côté. 2004. Structural and functional conservation of the NuA4 histone acetyltransferase complex from yeast to humans. *Mol. Cell. Biol.* 24:1884–1896. doi:10.1128/MCB.24.5.1884-1896.2004

Ferreira, H., J. Somers, R. Webster, A. Flaus, and T. Owen-Hughes. 2007. Histone tails and the H3 alphaN helix regulate nucleosome mobility and stability. *Mol. Cell. Biol.* 27:4037–4048. doi:10.1128/MCB.02229-06

Fuchs, M., J. Gerber, R. Drapkin, S. Sif, T. Ikura, V. Ogryzko, W.S. Lane, Y. Nakatani, and D.M. Livingston. 2001. The p400 complex is an essential E1A transformation target. *Cell.* 106:297–307. doi:10.1016/S0092-8674(01)00450-0

Galanty, Y., R. Belotserkovskaya, J. Coates, S. Polo, K.M. Miller, and S.P. Jackson. 2009. Mammalian SUMO E3-ligases PIAS1 and PIAS4 promote responses to DNA double-strand breaks. *Nature.* 462:935–939. doi:10.1038/nature08657

Gévry, N., H.M. Chan, L. Laflamme, D.M. Livingston, and L. Gaudreau. 2007. p21 transcription is regulated by differential localization of histone H2A.Z. *Genes Dev.* 21:1869–1881. doi:10.1101/gad.1545707

Goodarzi, A.A., A.T. Noon, D. Deckbar, Y. Ziv, Y. Shiloh, M. Löbrich, and P.A. Jeggo. 2008. ATM signaling facilitates repair of DNA double-strand breaks associated with heterochromatin. *Mol. Cell.* 31:167–177. doi:10.1016/j.molcel.2008.05.017

Gorrini, C., M. Squatrito, C. Luise, N. Syed, D. Perna, L. Wark, F. Martinato, D. Sardella, A. Verrecchia, S. Bennett, et al. 2007. Tip60 is a haplo-insufficient tumour suppressor required for an oncogene-induced DNA damage response. *Nature.* 448:1063–1067. doi:10.1038/nature06055

Hickson, I., Y. Zhao, C.J. Richardson, S.J. Green, N.M. Martin, A.I. Orr, P.M. Reaper, S.P. Jackson, N.J. Curtin, and G.C. Smith. 2004. Identification and characterization of a novel and specific inhibitor of the ataxia-telangiectasia mutated kinase ATM. *Cancer Res.* 64:9152–9159. doi:10.1158/0008-5472.CAN-04-2727

Hockemeyer, D., F. Soldner, C. Beard, Q. Gao, M. Mitalipova, R.C. DeKelver, G.E. Katibah, R. Amora, E.A. Boydston, B. Zeitler, et al. 2009. Efficient targeting of expressed and silent genes in human ESCs and iPSCs using zinc-finger nucleases. *Nat. Biotechnol.* 27:851–857. doi:10.1038/nbt.1562

Huen, M.S., R. Grant, I. Manke, K. Minn, X. Yu, M.B. Yaffe, and J. Chen. 2007. RNF8 transduces the DNA-damage signal via histone ubiquitylation and checkpoint protein assembly. *Cell.* 131:901–914. doi:10.1016/j.cell.2007.09.041

Ikura, T., S. Tashiro, A. Kakino, H. Shima, N. Jacob, R. Amunugama, K. Yoder, S. Izumi, I. Kuraoka, K. Tanaka, et al. 2007. DNA damage-dependent acetylation and ubiquitination of H2AX enhances chromatin dynamics. *Mol. Cell. Biol.* 27:7028–7040. doi:10.1128/MCB.00579-07

Jha, S., E. Shibata, and A. Dutta. 2008. Human Rvb1/Tip49 is required for the histone acetyltransferase activity of Tip60/NuA4 and for the downregulation of phosphorylation on H2AX after DNA damage. *Mol. Cell. Biol.* 28:2690–2700. doi:10.1128/MCB.01983-07

Kimura, H., and P.R. Cook. 2001. Kinetics of core histones in living human cells: little exchange of H3 and H4 and some rapid exchange of H2B. *J. Cell Biol.* 153:1341–1353. doi:10.1083/jcb.153.7.1341

Kolas, N.K., J.R. Chapman, S. Nakada, J. Ylanko, R. Chahwan, F.D. Sweeney, S. Panier, M. Mendez, J. Wildenhain, T.M. Thomson, et al. 2007. Orchestration of the DNA-damage response by the RNF8 ubiquitin ligase. *Science.* 318:1637–1640. doi:10.1126/science.1150034

Kruhlak, M.J., A. Celeste, G. Dellaire, O. Fernandez-Capetillo, W.G. Müller, J.G. McNally, D.P. Bazett-Jones, and A. Nussenzweig. 2006. Changes in chromatin structure and mobility in living cells at sites of DNA double-strand breaks. *J. Cell Biol.* 172:823–834. doi:10.1083/jcb.200510015

Kusch, T., L. Florens, W.H. Macdonald, S.K. Swanson, R.L. Glaser, J.R. Yates III, S.M. Abmayr, M.P. Washburn, and J.L. Workman. 2004. Acetylation by Tip60 is required for selective histone variant exchange at DNA lesions. *Science.* 306:2084–2087. doi:10.1126/science.1103455

Lee, J.H., and T.T. Paull. 2005. ATM activation by DNA double-strand breaks through the Mre11-Rad50-Nbs1 complex. *Science.* 308:551–554. doi:10.1126/science.1108297

Mailand, N., S. Bekker-Jensen, H. Faustrup, F. Melander, J. Bartek, C. Lukas, and J. Lukas. 2007. RNF8 ubiquitylates histones at DNA double-strand breaks and promotes assembly of repair proteins. *Cell.* 131:887–900. doi:10.1016/j.cell.2007.09.040

Mattera, L., F. Escaffit, M.J. Pillaire, J. Selves, S. Tyteca, J.S. Hoffmann, P.A. Gourraud, M. Chevillard-Briet, C. Cazaux, and D. Trouche. 2009. The p400/Tip60 ratio is critical for colorectal cancer cell proliferation through DNA damage response pathways. *Oncogene.* 28:1506–1517. doi:10.1038/onc.2008.499

Melander, F., S. Bekker-Jensen, J. Falck, J. Bartek, N. Mailand, and J. Lukas. 2008. Phosphorylation of SDT repeats in the MDC1 N terminus triggers retention of NBS1 at the DNA damage-modified chromatin. *J. Cell Biol.* 181:213–226. doi:10.1083/jcb.200708210

Morris, J.R., C. Boutell, M. Keppler, R. Densham, D. Weekes, A. Alamshah, L. Butler, Y. Galanty, L. Pangon, T. Kiuchi, et al. 2009. The SUMO modification pathway is involved in the BRCA1 response to genotoxic stress. *Nature.* 462:886–890. doi:10.1038/nature08593

Murr, R., J.I. Loizou, Y.G. Yang, C. Cuenin, H. Li, Z.Q. Wang, and Z. Herceg. 2006. Histone acetylation by Trrap-Tip60 modulates loading of repair proteins and repair of DNA double-strand breaks. *Nat. Cell Biol.* 8:91–99. doi:10.1038/ncb1343

Papamichos-Chronakis, M., J.E. Krebs, and C.L. Peterson. 2006. Interplay between Ino80 and Swr1 chromatin remodeling enzymes regulates cell cycle checkpoint adaptation in response to DNA damage. *Genes Dev.* 20:2437–2449. doi:10.1101/gad.1440206

Robert, F., S. Hardy, Z. Nagy, C. Baldeyron, R. Murr, U. Déry, J.Y. Masson, D. Papadopoulo, Z. Herceg, and L. Tora. 2006. The transcriptional histone acetyltransferase cofactor TRRAP associates with the MRN repair complex and plays a role in DNA double-strand break repair. *Mol. Cell. Biol.* 26:402–412. doi:10.1128/MCB.26.2.402-412.2006

Rubbi, C.P., and J. Milner. 2003. p53 is a chromatin accessibility factor for nucleotide excision repair of DNA damage. *EMBO J.* 22:975–986. doi:10.1093/emboj/cdg082

Samuelson, A.V., M. Narita, H.M. Chan, J. Jin, E. de Stanchina, M.E. McCurrach, M. Narita, M. Fuchs, D.M. Livingston, and S.W. Lowe. 2005. p400 is required for E1A to promote apoptosis. *J. Biol. Chem.* 280:21915–21923. doi:10.1074/jbc.M414564200

Sanders, S.L., M. Portoso, J. Mata, J. Bähler, R.C. Allshire, and T. Kouzarides. 2004. Methylation of histone H4 lysine 20 controls recruitment of Crb2 to sites of DNA damage. *Cell.* 119:603–614. doi:10.1016/j.cell.2004.11.009

Shechter, D., H.L. Dormann, C.D. Allis, and S.B. Hake. 2007. Extraction, purification and analysis of histones. *Nat. Protoc.* 2:1445–1457. doi:10.1038/nprot.2007.202

Shogren-Knaak, M., H. Ishii, J.M. Sun, M.J. Pazin, J.R. Davie, and C.L. Peterson. 2006. Histone H4-K16 acetylation controls chromatin structure and protein interactions. *Science.* 311:844–847. doi:10.1126/science.1124000

Shroff, R., A. Arbel-Eden, D. Pilch, G. Ira, W.M. Bonner, J.H. Petrini, J.E. Haber, and M. Lichten. 2004. Distribution and dynamics of chromatin modification induced by a defined DNA double-strand break. *Curr. Biol.* 14:1703–1711. doi:10.1016/j.cub.2004.09.047

Smerdon, M.J., T.D. Tlsty, and M.W. Lieberman. 1978. Distribution of ultraviolet-induced DNA repair synthesis in nuclease sensitive and resistant regions of human chromatin. *Biochemistry.* 17:2377–2386. doi:10.1021/bi00605a020

Spycher, C., E.S. Miller, K. Townsend, L. Pavic, N.A. Morrice, P. Janscak, G.S. Stewart, and M. Stucki. 2008. Constitutive phosphorylation of MDC1 physically links the MRE11-RAD50-NBS1 complex to damaged chromatin. *J. Cell Biol.* 181:227–240. doi:10.1083/jcb.200709008

Stewart, G.S., S. Panier, K. Townsend, A.K. Al-Hakim, N.K. Kolas, E.S. Miller, S. Nakada, J. Ylanko, S. Olivarius, M. Mendez, et al. 2009. The RIDDLE syndrome protein mediates a ubiquitin-dependent signaling cascade at sites of DNA damage. *Cell.* 136:420–434. doi:10.1016/j.cell.2008.12.042

Stiff, T., M. O'Driscoll, N. Rief, K. Iwabuchi, M. Löbrich, and P.A. Jeggo. 2004. ATM and DNA-PK function redundantly to phosphorylate H2AX after exposure to ionizing radiation. *Cancer Res.* 64:2390–2396. doi:10.1158/0008-5472.CAN-03-3207

Stucki, M., J.A. Clapperton, D. Mohammad, M.B. Yaffe, S.J. Smerdon, and S.P. Jackson. 2005. MDC1 directly binds phosphorylated histone H2AX to regulate cellular responses to DNA double-strand breaks. *Cell.* 123:1213–1226. doi:10.1016/j.cell.2005.09.038

Sun, Y., X. Jiang, S. Chen, N. Fernandes, and B.D. Price. 2005. A role for the Tip60 histone acetyltransferase in the acetylation and activation of ATM. *Proc. Natl. Acad. Sci. USA.* 102:13182–13187. doi:10.1073/pnas.0504211102

Sun, Y., Y. Xu, K. Roy, and B.D. Price. 2007. DNA damage-induced acetylation of lysine 3016 of ATM activates ATM kinase activity. *Mol. Cell. Biol.* 27:8502–8509. doi:10.1128/MCB.01382-07

Sun, Y., X. Jiang, Y. Xu, M.K. Ayrapetov, L.A. Moreau, J.R. Whetstine, and B.D. Price. 2009. Histone H3 methylation links DNA damage detection to activation of the tumour suppressor Tip60. *Nat. Cell Biol.* 11:1376–1382. doi:10.1038/ncb1982

Tóth, K., N. Brun, and J. Langowski. 2006. Chromatin compaction at the mononucleosome level. *Biochemistry.* 45:1591–1598. doi:10.1021/bi052110u

Tsukuda, T., A.B. Fleming, J.A. Nickoloff, and M.A. Osley. 2005. Chromatin remodelling at a DNA double-strand break site in *Saccharomyces cerevisiae*. *Nature.* 438:379–383. doi:10.1038/nature04148

Urnov, F.D., J.C. Miller, Y.L. Lee, C.M. Beausejour, J.M. Rock, S. Augustus, A.C. Jamieson, M.H. Porteus, P.D. Gregory, and M.C. Holmes. 2005. Highly efficient endogenous human gene correction using designed zinc-finger nucleases. *Nature.* 435:646–651. doi:10.1038/nature03556

van Attikum, H., O. Fritsch, B. Hohn, and S.M. Gasser. 2004. Recruitment of the INO80 complex by H2A phosphorylation links ATP-dependent chromatin remodeling with DNA double-strand break repair. *Cell.* 119:777–788. doi:10.1016/j.cell.2004.11.033

von Holt, C., W.F. Brandt, H.J. Greyling, G.G. Lindsey, J.D. Retief, J.D. Rodrigues, S. Schwager, and B.T. Sewell. 1989. Isolation and characterization of histones. *Methods Enzymol.* 170:431–523. doi:10.1016/0076-6879(89)70061-6

Wang, X., and J.J. Hayes. 2008. Acetylation mimics within individual core histone tail domains indicate distinct roles in regulating the stability of higher-order chromatin structure. *Mol. Cell. Biol.* 28:227–236. doi:10.1128/MCB.01245-07

Yang, Y., Y. Kuang, R. Montes De Oca, T. Hays, L. Moreau, N. Lu, B. Seed, and A.D. D'Andrea. 2001. Targeted disruption of the murine Fanconi anemia gene, Fancg/Xrcc9. *Blood.* 98:3435–3440. doi:10.1182/blood.V98.12.3435

Zhong, H., A. Bryson, M. Eckersdorff, and D.O. Ferguson. 2005. Rad50 depletion impacts upon ATR-dependent DNA damage responses. *Hum. Mol. Genet.* 14:2685–2693. doi:10.1093/hmg/ddi302

Ziv, Y., D. Bielopolski, Y. Galanty, C. Lukas, Y. Taya, D.C. Schultz, J. Lukas, S. Bekker-Jensen, J. Bartek, and Y. Shiloh. 2006. Chromatin relaxation in response to DNA double-strand breaks is modulated by a novel ATM- and KAP-1 dependent pathway. *Nat. Cell Biol.* 8:870–876. doi:10.1038/ncb1446